Transportation Research Part C 93 (2018) 396–409

Contents lists available at ScienceDirect

Transportation Research Part C

journal homepage: www.elsevier.com/locate/trc

Probabilistic risk analysis of flying ballast hazard on high-speed rail lines

Jieyi Deng[a], Xiang Liu[a,*], Guoqing Jing[b], Zheyong Bian[a]

[a] Department of Civil and Environmental Engineering, Rutgers, The State University of New Jersey, United States
[b] Department of Highway and Railway Engineering, Beijing Jiaotong University, China

ARTICLE INFO

Keywords:
High-speed rail
Flying ballast
Safety
Risk analysis

ABSTRACT

Flying ballast is a significant safety concern for high-speed train operations on ballasted tracks. It is the phenomenon of a ballast particle displaced from the track, due to the aerodynamic force induced by a passing train traveling above a certain speed. Flying ballast can potentially damage tracks and rolling stock, thereby posing a risk to high-speed rail operations. This paper develops a Probabilistic Risk Analysis (PRA) model based on the information available from the field and the literature. The model enables a quantitative assessment of the probability of ballast particle displacement at a particular position on the track, as well as the probabilistic distribution of the total number of ballast particles that are expected to move. The model accounts for various risk factors, such as train speed, ballast gradation, and track position. The model application is illustrated using a ballasted track on the Yellow River Bridge on the Beijing-Shanghai high-speed rail line in China. The analysis finds that flying ballast probability increases when train speed increases, in particular, the problem of flying ballast becomes more pronounced when train speed exceeds 350 km per hour (217 miles per hour). Flying ballast probability might be reduced when the ballast profile is lower, given all else being equal. In addition, flying ballast probability is expected to be higher at the center of the track than in other positions. The proposed risk model can be further developed and ultimately be used to evaluate route-specific flying ballast risk, enabling the identification, assessment, and comparison of risk mitigation strategies in order to support emerging high-speed rail operations.

1. Introduction

High-speed rail (HSR) delivers a safe, fast and energy-efficient means for long distance passenger transportation. Given the development of global HSR systems in recent years, operational safety is of crucial importance.

Flying ballast (defined as displaced ballast particles in this paper) is a primary safety concern for HSR operations on ballasted tracks. Flying ballast can cause damage to locomotives, railcars, and tracks, and may even injure workers near tracks, resulting in significant economic losses and safety hazards. Therefore, understanding and managing flying ballast risk is vital for assuring HSR operational safety.

Ballast flight occurs on ballasted tracks, which can have a range of impacts, from minor to consequential. In addition to ballasted tracks, another common track type in HSR system is called non-ballasted track (also known as Slab Track) (Fig. 1). Non-ballasted track usually provides high longitudinal and lateral stability (Steenbergen et al., 2007). Non-ballasted track has been used extensively, such as on new lines in the Chinese HSR network and Japanese Shinkansen network (Esveld, 2003). Although non-ballasted

* Corresponding author.
E-mail address: xiang.liu@rutgers.edu (X. Liu).

https://doi.org/10.1016/j.trc.2018.06.003
Received 16 December 2017; Received in revised form 9 May 2018; Accepted 7 June 2018

Fig. 1. Ballasted track and non-ballasted track.

track has been put to use on new HSR lines, many existing HSR lines still use ballasted tracks due to various economic and technological challenges preventing the replacement of all ballasted tracks with non-ballast tracks. In addition, ballasted track has its advantages in terms of lower capital cost and long-term maintenance convenience (Indraratna et al., 2011). Moreover, non-ballasted track cannot be used in certain areas, such as those prone to earthquakes or with softer soil (Saat et al., 2015). For these reasons, ballasted track is still used on many HSR lines; for example, in France, Italy and Spain, dominant HSR track structure remains ballast bed, and thus these tracks are open to the risk of flying ballast.

This paper focuses on evaluating flying ballast risk on ballasted tracks for HSR operations. Although several alternative risk mitigation strategies have been identified in the literature, there is no integrated risk analysis framework through which alternative risk mitigation strategies can be evaluated and compared. The current practice is still mostly reliant on engineering experience. With the aim of advancing both the state of the art and the current practice with respect to flying ballast risk management, this paper develops a Probabilistic Risk Analysis (PRA) model to estimate the probability distribution of the number of flying ballast particles given different operating conditions and at different track positions. PRA is a useful technique for assessing the risk of a rare event (Paté-Cornell and Dillon, 2001). Because of the low occurrence probability of flying ballast, direct statistical analysis is not suitable due to the limited sample size. Instead, PRA decomposes a rare event into a chain of events and influencing factors, and then integrates them using probabilistic methods. PRA has been used in various safety-critical engineering domains, such as space shuttles, nuclear facilities, and aviation (Paté-Cornell, 2002; Paté-Cornell and Dillon, 2001; Vesely and Rasmuson, 1984; Garrick and Christie, 2002; Mohaghegh et al., 2009).

In the context of flying ballast, the mechanism of its occurrence can be described using a mechanistic model accounting for various forces (e.g. interlock force, aerodynamic force, vibration force). The forces leading to a ballast flight can be affected by specified infrastructure factors (e.g. ballast gradation, ballast height) or operational factors (e.g. train speed). When some of these factors are uncertain at the time of risk analysis, PRA can be used as a systematic approach to propagate these factor-specific uncertainties to derive the uncertainty of flying ballast. In this paper, the risk is defined as the probability distribution of the number of flying ballast particles. With the help of the PRA model, the risk analysis methodology is built upon an understanding of the phenomenon and mechanism of ballast flight occurrence, and accounts for a variety of operating and infrastructure characteristics in the field. The general methodology can be adapted to specific routes or networks. The ultimate goal is to evaluate location-oriented flying ballast risk, thereby understanding the effectiveness of potential risk mitigation strategies for HSR safety assurance on specific ballasted tracks.

The remainder of this paper is structured as follows: Section 2 provides a review of previous research in related fields. Section 3 identifies the knowledge gaps that this research aims to narrow. Section 4 estimates flying ballast probabilities under different operational circumstances. A case study of a section of high-speed rail line in China is developed in Section 5, to illustrate model application. Finally, the significant contributions, limitations of this research, and a future research plan are discussed in Sections 6–8.

2. Literature review

Previous studies have focused on understanding the process and influencing factors related to flying ballast in HSR operations. As Table 1 shows, the prior methods include field tests, mechanistic models, risk assessment methods and common risk reduction strategies in practice. Based on these approaches, previous studies identify promising risk mitigation strategies.

2.1. Field experiments

Several field experiments have been performed in order to understand the physical characteristics of ballast flight and relevant aerodynamic factors. For instance, Kwon and Park (2006) conducted a field investigation based on the shape and mass of ballast particles in order to explore the relationship between train velocity and airflow speed underneath the train. The probability of ballast

Table 1
A high-level summary of related literature.

	Description	Advantages	Limitations	References
Field experiment	Used in-situ experiments to understand the physical characteristics of ballast flight and relevant aerodynamic factors	Controlled environment to isolate the effect of studied factor; represent actual operating conditions	Capital and labor-intensive; specific to certain locations	Baker (2010), Kwon and Park (2006), Quinn et al. (2010), Cali and Covert (2000), Quinn et al. (2001), Lazaro et al. (2011), Pita (2001), Morgan and Markland (1981), Prud (1970), Ferreira (2014)
Mechanistic model	Used analytical or simulation methods to understand the mechanism of flying ballast	Mathematically describe the physical mechanism of flying ballast	Limited by the understanding of the mechanism, and may be restrained by computational resources or data availability	Jacobini et al. (2013), Jing et al. (2012), Lazaro et al. (2011), Saussine et al. (2011)
Risk assessment	Qualitative and quantitative risk assessment methods were used	Account for both probability and consequence of flying ballast, and consider various influencing factors	The prior work does not address the distribution of the number of flying ballast particles; also the prior risk model is limited to certain assumptions and selected factors	Kwon and Park (2006), Jacobini et al. (2013), Quinn et al. (2010), Lazaro et al. (2011), Saussine et al. (2011), Saussine et al. (2015)
Risk mitigation strategies	Identified various engineering and operational solutions to mitigate flying ballast risk (e.g. lowering ballast profile, lowering ballast shoulder or speed reduction)	Identified ways to mitigate flying ballast risk based on its occurrence mechanism	There is no integrated framework to compare these strategies, individually or in combination; little comprehensive analysis of cost-effectiveness	Kown et al. (2006), Saussine et al. (2013), Saat et al. (2015), Esveld et al. (2001), Esveld (2003), Indraratna et al. (2011)

flight during the passage of a high-speed train was assessed by comparing the results from a wind tunnel test and those from field measurements. Quinn and Hayward (2008) conducted an in-situ experiment in the United Kingdom to monitor the condition of the pressure coefficient and measure the aerodynamic forces exerted on a suspended ballast particle. They also conducted another study to investigate the cause of the movement of ballast particles (Quinn et al., 2010). In this study, empirical observations to understand airflow behavior during train passage were performed. Baker (2010) presented an aerodynamic assessment of train underbody flow. Lazaro et al. (2011) analyzed the ballast flight phenomenon on the Madrid Barcelona high-speed line. A series of devices were installed on a portion of HSR lines to measure the aerodynamic pressure induced by the passage of a high-speed train.

2.2. Mechanistic models

The mechanisms related to ballast flight are complex, involving train dynamic response from sleeper interaction and aerodynamic force (Jing et al., 2012; Jacobini et al., 2013; Saat et al., 2015). Jacobini et al. (2013) presented a list of possible factors that may contribute to flying ballast risk. These factors include: train aerodynamics, track responses, ground effects, and atmospheric conditions. Based on a semi-quantitative risk analysis approach, Jing et al. (2012) described the relationship between the macroscopic appearance and the microscopic force analysis for ballast particles. Comparing the most common mechanisms, they considered the track vibration generated by train passage and aerodynamic force as the major causes of ballast displacement.

2.3. Risk assessment

Most previous studies either used in-situ experiments (e.g., Cali and Covert, 2000; Kwon and Park, 2006; Baker, 2010; Quinn and Hayward, 2008; Quinn et al., 2010), mechanistic models such as aerodynamic modeling and CFD simulation modeling (e.g., Lazaro et al., 2011; Jing et al., 2012; Saat et al., 2015), or risk assessment models (e.g., Jacobini et al. 2013; Saat et al., 2015; Saussine et al., 2011, 2015) to analyze the hazards posed by ballast flight on HSR lines. In particular, with respect to risk assessment, Kwon and Park (2006) developed a ballast flight probability factor based on train speed and ballast mass. However, that study did not account for the interactions among ballast particles, particularly ballast interlocking forces. Later, Saussine et al. (2011) proposed a Stress-Strength Interference Analysis to estimate flying ballast probability accounting for train speed as well as track resistance. Their model assumed that both strength and stress variables follow normal distributions. Also, their model does not provide the probability distribution of the number of flying ballast. Our proposed model contributes to the body of knowledge in the following ways:

(1) Our proposed PRA model can estimate the probability distribution of any number of flying ballasts. Given all else being equal, more ballast particles being prone to flight may indicate a greater hazard to train operational safety.
(2) Our PRA model is more flexible, and it can incorporate any type of variable distributions.
(3) Our model is built upon the mechanistic analysis of the ballast flight mechanism, and describes the relationship between flying ballast risk with specific operating factors (e.g., ballast height, mass, train speed).

2.4. Risk mitigation strategies

Previous studies have identified several risk mitigation strategies (two selected examples are shown in Fig. 2). Based on the research conducted at the Korea Railroad Research Institute (Kwon and Park, 2006), a lowered ballast surface would be a possible solution to reduce flying ballast risk. The closer to the underbody of the train, the higher the aerodynamic wind pressure, and the higher probability of a ballast flight, given all else being equal. If the ballast surface is lower, there would be fewer particles within range to fly. For the central part of the track, lowering the ballast profile means reducing the height of the ballast by removing extra particles on the surface. In addition, speed reduction is another risk reduction option. According to Saussine et al. (2013), in France and other countries, there are provisions that mandate temporary speed reductions during bad weather conditions (Saussine et al.,

a) Ballast profile lowered on the Rome-Naples HSR b) Ballast Bagging, the solution proposed in Shinkansen, Japan

Fig. 2. Examples of risk mitigation strategies.

2013). Although the speed reduction is a potential mitigation strategy for flying ballast risk mitigation, this solution also affects HSR operational efficiency (Saat et al., 2015).

Other strategies, such as ballast bagging, glue bonding, and installing novel sleepers or slab tracks on newly developed high-speed lines, are alternative engineering solutions, but also have drawbacks in terms of life-cycle maintenance and performance over the lifetime of HSR lines (Indraratna et al., 2011; Esveld et al., 2001). According to Saat et al. (2015), different risk mitigation strategies have respective advantages and disadvantages. For example, ballast bagging is a normal form of management for the ballasted track of Shinkansen lines in Japan (Esveld, 2003). This solution is effective because the particles are contained with netting; on the other hand, the bags need to be removed and replaced for track maintenance, which is labor-intensive and costly. All risk mitigation strategies are developed based on an understanding of the flying ballast mechanism and influencing factors (Saat et al., 2015). In practice, it is important to quantitatively evaluate flying ballast risk given specified operational conditions, in order to compare and implement effective risk mitigation strategies under specific circumstances. However, there is no integrated framework to compare these strategies, individually or in combination, and there is little comprehensive analysis of cost-effectiveness.

3. Knowledge gaps and intended research contributions

Most of the prior research in this field has focused on the relationship between the mechanistic variables (e.g., aerodynamic force) and flying ballast risk. This “micro-level” risk assessment is useful for engineering studies when detailed information is available. However, very few studies have accounted for the link between operating characteristics (e.g. speed, ballast height) and those mechanistic variables, and thus the risk. For instance, if we apply speed reduction as a potential risk reduction strategy, we need to know how speed can affect the aerodynamic factors that directly affect flying ballast probability.

In practice, for “macro-level” risk planning, the exact values of those mechanistic variables might not be available but could be inferred based on operating variables (e.g. speed, track type, train type, ballast gradation). For risk planning purposes, a “macro-level” risk assessment model is more suitable in order to estimate the level of risk caused by different infrastructure and operational characteristics, in lieu of equipping specialized monitoring systems along rail lines to measure those mechanistic variables in real time. In addition, the “macro-level” risk assessment focuses on the variables that decision makers can change (e.g. speed reduction or lowering ballast profile). Therefore, this paper focuses on “macro-level” risk assessment based on HSR operating factors. The model can be used as a risk evaluation and comparative approach for ballasted tracks. The model will be built upon the mechanistic analysis of the ballast flight mechanism and describes the relationship between specific operating factors of flying ballast risk (e.g. ballast height, train speed). The risk model might later be implemented into a decision support framework that helps railroad engineers evaluate the change of risk in response to the change of certain operating parameters, and thus prioritize the allocation of limited safety resources. Note that each risk reduction strategy has its own implementation cost and may also affect infrastructure and train operations. Nonetheless, a detailed cost-benefit analysis is beyond the scope of this work but will be treated as a separate study in the future.

4. Methodology

In general, risk is defined as the probability distribution of the consequence of an event (Kaplan and Garrick, 1981). Probabilistic risk assessment (PRA) focuses on estimating the probability of an event and its consequence. In the context of flying ballast risk analysis, the risk can be defined as the probability distribution of the number of ballast particles that move in a vertical direction, which is primarily the consequence of sufficient longitudinal momentum. Both horizontal and vertical movement of ballast can cause damage to track infrastructure and rolling stock. This paper focuses on the ballast flight in the vertical direction. Horizontal movement, also called ballast fluidization, has a different mechanism and needs to be studied in a separate future study.

In this paper, we use the number of ballast flights as a proxy variable to indicate the consequence of flight ballast. Given all else being equal, more flying particles could introduce more opportunities to damage rolling stock and track, as well as track workers along the track line. We estimate its probability of occurrence for each possible number of flying ballast particles. The actual consequence would be complex and subject to many factors on the site. Future research can be developed to further adapt the risk model to any specific measures of risk (e.g. monetary damage cost, injuries). As stated earlier, the mechanism of flying ballast occurrence accounts for various factors, each of which is subject to uncertainty at the time of risk analysis. For example, when we perform a risk assessment of flying ballast on a line, the actual aerodynamic force is uncertain but can be estimated using a probabilistic distribution. The probability distribution of this variable can be developed based on field observations (Quinn et al., 2010; Cheli et al., 2007; Kwon, 2010; Pita, 2001). The integration and risk propagation of these uncertainties are conducted using Monte Carlo simulation in the PRA framework. Thus, with the help of the PRA model, the risk analysis methodology is built upon an understanding of the phenomenon and mechanism of ballast flight occurrence, and accounts for a variety of operating and infrastructure characteristics in the field. The general methodology can then be adapted to specific routes or networks.

4.1. Mechanism of ballast flight

In order to assess the probability of ballast flight, previous studies (Luo et al., 1996; Saussine et al., 2011; Jing et al., 2012; Jacobini et al., 2013) have analyzed the mechanism process of ballast flight and a preliminary list of possible risk factors that may contribute to flying ballast. An illustrative mechanism of ballast flight appears in Fig. 3 (Jing et al., 2012).

As shown above, the mechanical system of a ballast particle is balanced by four types of force, including gravitational force,

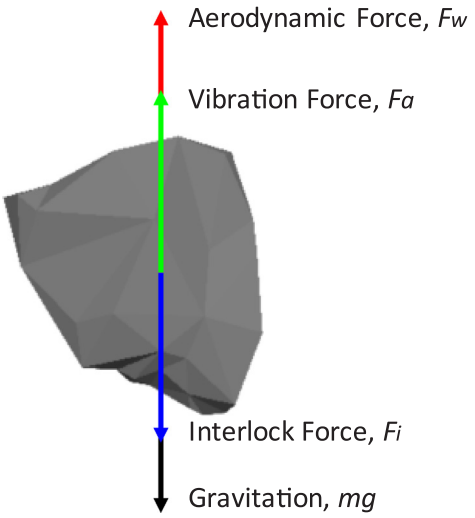

Fig. 3. Schematic ballast flight mechanic equilibrium (Jing et al., 2012).

interlock force, aerodynamic force, and vibration force. The initial balanced mechanical relationship can be expressed as:

$$F_w + F_a = mg + F_i \tag{1}$$

where:

F_w = aerodynamic force
F_a = vibration force
mg = gravitational force
F_i = interlock force.

Once the system balance is broken, the particle will gain a resultant force in a vertical direction; thus, the particle will transit from a static situation to a dynamic state, which will lead to the ballast displacement. This displacement is referred to "flying ballast" in this study.

Eq. (1) can be re-written as follows:

$$F = (F_w + F_a) - (mg + F_i) \tag{2}$$

F is the net vertical resultant force caused by HSR train passage. Eq. (2) is named as the "limit state function" (Jing et al., 2012), representing the critical state of ballast. The next section introduces a probabilistic risk model to evaluate the probability of ballast flight.

4.2. PRA model

Several studies have discussed mechanistic variables, such as the friction and aerodynamic force from laboratory testing or in-field experiments. Most of the mechanistic variables are related to operating parameters such as train speed, particle gradation,

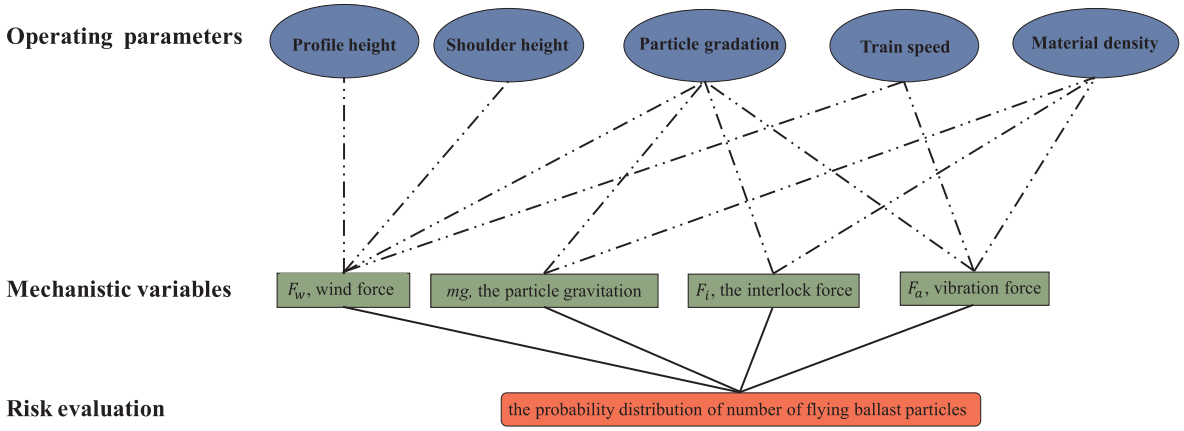

Fig. 4. The relationship between operating variables, mechanistic variables and flying ballast risk.

Table 2
Operating variables considered in this paper.

Operation parameters	Description
V_{train}	HSR train speed (km/h)
$l_{gradation}$	Distribution of ballast diameter
$\rho_{ballast}$	The material density of ballast
$H_{shoulder}$	Ballast shoulder height at the end of tie (m)
$H_{profile}$	The height difference between ballasted bed and tie (m)

profile height, and sleeper types (Fig. 4).

The mechanistic variables (F_w, F_a, mg, F_i) would be affected by a set of operating variables. However, due to data limitation, we mainly discuss the variables listed in Table 2. Additional factors will be considered in our future work. Furthermore, given specified operating variables, the mechanistic forces are also subject to uncertainties which can be represented by probability distributions. The probability distributions are estimated based on either laboratory testing or in-field observations (Jing et al., 2012; Quinn et al., 2010; Cheli et al., 2007; Kwon, 2010).

The relationship between each operating parameter and its corresponding mechanistic variable(s) is discussed in the following sections.

Ballast mass (mg)

The distribution of the particle mass is generated based on Eq. (3). In particular, the particle is viewed as a cube equivalent to the size of the particle(Jing et al., 2012; Shao et al., 2016). The mass of the particle can be calculated as follows:

$$mg = l^3 \times \rho_{ballast} \times g \tag{3}$$

where:

mg = ballast mass, N

l = the size of the particle, m

$\rho_{ballast}$ = the material density of the ballast particle, kg/m^3

g = gravity acceleration, N/kg.

The particle gradation in engineering describes the specific distribution of the ballast particle size on specific rail lines. As a result, the final mass distribution of the ballast is shaped like a normal distribution $mg \sim N(\mu_{mg}, \sigma_{mg})$.

Interlock force (F_i)

The dynamic ballast interlock force is difficult to estimate, but the static forces can be used to measure the ballast particle interlock ability. According to Jing et al. (2012), interlock force is influenced by particle compactness, usually no more than 20% of the weight. As per Shao et al. (2016), the interlock force is assumed to be approximately 10% of the weight.

Aerodynamic force (F_w)

According to the aerodynamic features of the airflow around fast moving vehicles, the aerodynamic wind pressure varies significantly at different locations along the track (Cali and Covert, 2000; Quinn et al., 2001, 2010; Soper et al., 2017). Based on the prior research, aerodynamic wind pressure varies by ballast shoulder height. Similarly, the aerodynamic force also varies by profile height. Ballast profile height, shoulder height and train speed are all considered in the calculation of aerodynamic force.

For F_w, the distributions of the load stress are greatly influenced by aerodynamic factors. The aerodynamic force is generated by a generic formula described in ASCE (1994).

$$F_a = A \times \alpha \times P_{air} \tag{4}$$

where:

F_w = aerodynamic force, N

A = effective contact surface of the particle, m^2

α = aerodynamic wind coefficient

P = air pressure, N/m^2

As for the effective contact surface A, we use the particle size to calculate the area:

$$A = l^2 \tag{5}$$

Thus, the final expression of the aerodynamic force is:

$$F_w = l^2 \times \alpha \times P_{air} \tag{6}$$

Referring to Baker (2014), the aerodynamic wind coefficient (α) is strongly influenced by the passage duration depending on the length of the train and the velocity. In the ballasted high-speed railway system, we utilize the recorded in-situ experiment data (Quinn et al., 2010) to estimate the aerodynamic wind coefficient (α).

From the perspective of aerodynamics, air pressure is directly influenced by the aerodynamic wind velocity underneath the train, which is then influenced by the train velocity (Kwon and Park, 2006). In the experiments that give the train speed and aerodynamic wind velocity, the variation of the air pressure was recorded.

Vibration (F_a)

Another influencing factor for ballast flight is the ballast bed vibration (Jing et al., 2012). In this case, the relationship between the acceleration caused by the ballast bed vibration and corresponding force is defined as follows:

$$F_a = ma_V \tag{7}$$

where: a_V = acceleration, m/s^2

m = weight of the particle, kg

According to some previous experimental laboratory studies (Prud, 1970; Morgan and Markland, 1981; Pita, 2001), ballast flight risk increases with more significant ballast bed vibration. Due to data limitations, we do not have the exact distribution of ballast acceleration accounting for all location-specific characteristics. Therefore, we assumed 1.4 g in this paper based on the prior literature (Gao et al., 2017; Mishra et al., 2014; Pita, 2001). This value, which appears to be within the reasonable range based on the literature review, is used to illustrate our PRA methodology. When other vibration values are used, the results can be updated accordingly. Depending on the specific operating variables, the value of the vibration force can be expressed by Eq. (8).

Based on the four forces described above (aerodynamic force, vibration force, interlock force and gravitational force), the ballast force equilibrium can be rewritten as:

$$F = (l^2\alpha P_{air} + ma_V) - (mg + 0.1mg) = l^2\alpha P_{air} + (a_V - 1.1g)\rho_{ballast} l^3 \tag{8}$$

As discussed before, the balanced system would be broken once the resultant force is greater than zero. With this model, the probabilistic risk of ballast flight can be directly linked to the operating factors, including aerodynamic wind velocity V_{wind}, ballast gradation (particle size distribution) l, and ballast material density $\rho_{ballast}$. Moreover, aerodynamic wind velocity is greatly influenced by train speed (Kwon and Park, 2006). Accordingly, the probabilistic risk of ballast flight can be generally expressed as:

$$P_f = \int_0^{+\infty} f(F)dF \tag{9}$$

where, function $f(F)$ is the probability density of resultant force F in Eq. (9).

Because the above-mentioned variables can follow any probabilistic distributions, we use Monte-Carlo simulation as a general approach to estimate the probability of ballast movement accounting for specific types of variable distributions. The developed pseudo-code of the probabilistic model is presented in Fig. 5.

Especially according to previous related work (Shao et al., 2016; Saussine et al., 2015), the aerodynamic variables can be defined as Gaussian probability density functions.

5. Case study

A numerical example is developed to demonstrate the application of the proposed risk model in assessing flying ballast risk. Based on the proposed risk model, we estimate and compare the impacts of alternative risk reduction options, including (1) speed reduction, (2) lowering ballast profile, and (3) lowering ballast shoulder height. In this case, a 728-meter (0.5 mile) ballasted track segment from one HSR line in China is taken as an example. The ballast gradation information on this segment is provided by the Ministry of China Railway. We aim to estimate the magnitude of flying ballast risks associated with different combinations of speeds, ballast profile

Monte-Carlo simulation for probabilistic assessment of flying ballast

1: Initialize chosen operating parameters, including the train velocity V_{train}, ballast diameter distribution $l_{gradation}$, particle density $\rho_{ballast}$, the ballast shoulder height $H_{shoulder}$ and the ballast profile height $H_{profile}$.
2: Initialize the corresponding distribution characters (μ_i, σ_i) of each force variable, given specific influencing operating variables.
3: Initialize f(x)=0
4: **for** $i = 1{:}\,nit$
5: $mg = rand(\mu_{mg}, \sigma_{mg})$
6: $F_i = rand(\mu_{F_i}, \sigma_{F_i})$
7: $F_w = rand(\mu_{F_w}, \sigma_{F_w})$
8: $F_a = rand(\mu_{F_a}, \sigma_{F_a})$
9: $F = (F_w + F_a) - (mg + F_i)$
10: **if** $F > 0$ then
11: $n = n + 1$
12: **end if**
13: **end for**
14: $P_f = n/nit$
15: Output (P_f)

Fig. 5. Monte Carlo simulation for estimating the flying probability of a ballast particle.

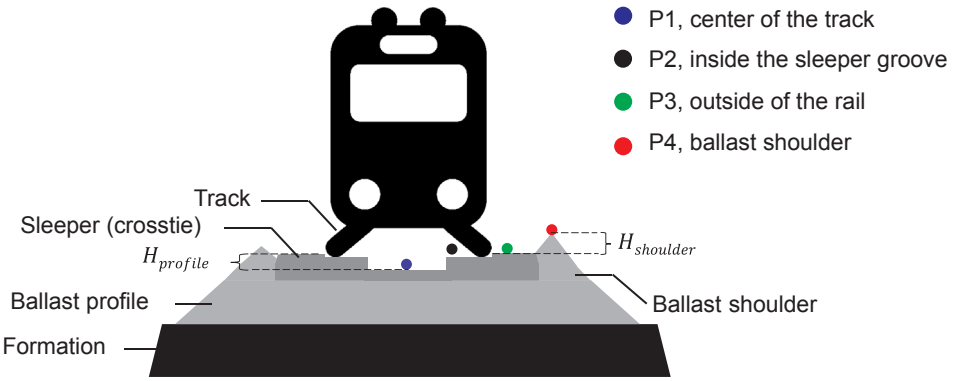

Fig. 6. Schematic diagram of track model and the points of interest on the track.

heights, ballast shoulder heights and track positions. We want to understand the range of risk given various factors in combination. Not all the scenarios considered in our risk illustration examples have been implemented in practice due to other engineering considerations.

5.1. Description of operational scenario

Four positions on the track section are selected as the points of interest, which may exhibit different aerodynamic forces during the passage of trains. Based on in-situ experiments (Jing et al., 2012), these points of interest are named based on their locations on the track. Point 1(P1) is located in the center of the track, Point 2 (P2) is located inside the sleeper groove, and Point 3 (P3) is in the opposite position outside of the rail. Point 4 (P4) is at the top of the ballast shoulder (Fig. 6).

5.2. Baseline risk

Assume that a train is traveling from 250 km/h (155 mph) to 400 km/h (249 mph) on the HSR lines. As discussed previously, 300 km/h is usually recognized as the cutoff point for ballast flight occurrence. However, an increase of the speed to 350 km/h is considered a development demand for high-speed trains in practice (Premoli et al., 2015; Saussine et al., 2015). Thus, the scenario with a velocity of 350 km/h is designed as the baseline scenario in further discussion. Fig. 7 shows the probabilistic distributions of the number of flying ballast particles at each point of interest (P1, P2, P3 and P4). Fig. 7 also presents the average (mean) number of flying ballast particles for one train passing the studied HSR section. This probability distribution is estimated based on the total number of ballast placed along the track, as well as the probability of flight for each ballast particle.

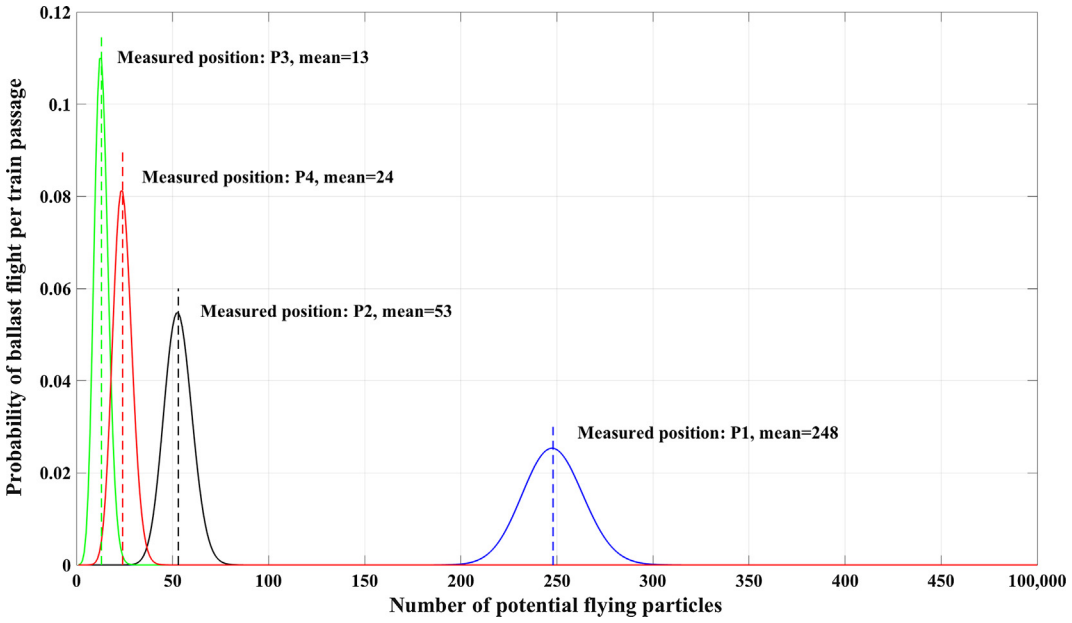

Fig. 7. Probabilistic distribution of the number of ballast flight per train passage, V_{train} = 350 km/h.

Table 3
Parameters in the sensitivity analysis.

Scenario simulation	Operating parameter setting	
Baseline	Measured position: P1 ~ P4	$H_{profile}$ = 0 m
	V_{train} = 350 km/h	$H_{shoulder}$ = 0.15 m
Speed reduction	Measured position: P1	$H_{profile}$ = 0 m
	V_{train} = 250 km/h ~ 400 km/h	$H_{shoulder}$ = 0.15 m
Lowering ballast profile	Measured position: P1	$H_{profile}$ = −0.04 m
	V_{train} = 350 km/h	$H_{shoulder}$ = 0.15 m
Lowering ballast shoulder	Measured position: P4	$H_{profile}$ = 0 m
	V_{train} = 350 km/h	$H_{shoulder}$ = 0 m

P1 is the location where ballast flight is most likely to occur among all of the four locations. This result is supported by in-situ observations. Based on the related discussions (Quinn and Hayward, 2008; Baker, 2014; Saat et al., 2015), the aerodynamic wind velocity and sleeper vibration in the center area can greatly influence the balance of ballast particles within this scope. Therefore, all of the following discussions will focus on the P1 position, which is on the centerline of the HSR track.

The next step is to estimate the mean number of potential ballast flights with different risk mitigation strategies. By applying the proposed risk assessment model with the risk mitigation techniques under specific scenarios, the effects of discussed risk mitigation methods can be compared.

5.3. Sensitivity analysis

We conduct a series of sensitivity analyses in order to understand the effect of influencing risk factors (speed, ballast depth) on flying ballast risk, which is represented by the mean number of flying ballast particles on the studied rail section. This analysis will provide information to identify, evaluate, and compare potential risk mitigation strategies.

Firstly, Table 3 presents the operation parameters in each scenario.

1) Effect of train speed

In this case, the train speeds are set as 250 km/h (155 mph), 300 km/h (186 mph), 350 km/h (217 mph) and 400 km/h (249 mph), which are the common speed levels used in HSR operation or design. For instance, the HSR operation speed in England and Russia has reached 400 km/h and caused severe safety concerns regarding ballast flight. Fig. 8 shows the estimated probability of different numbers of ballast flights in the center area (P1).

The risk of ballast flight becomes greater in the central area of the track section with increased speed. The results show that the risk of ballast flight increases sharply when the speed increases from 300 km/h to 350 km/h, which is consistent with the findings of

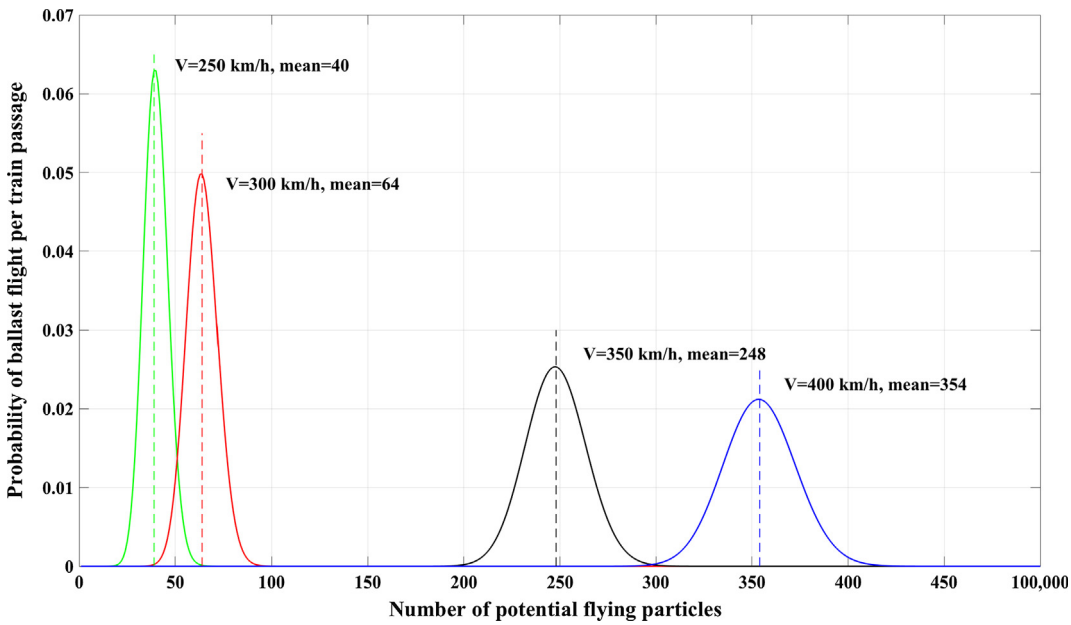

Fig. 8. Distribution of the number of ballast flights per train passage (center line of track, P1 position).

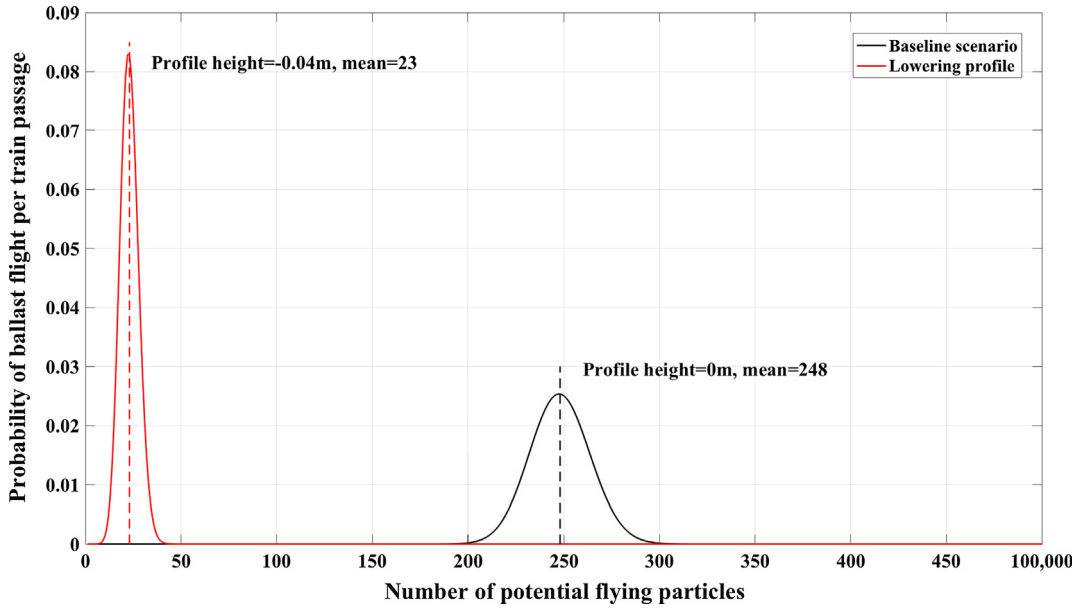

Fig. 9. Distribution of the number of ballast flight per train passage for track centerline, P1.

prior studies (Saat et al., 2015; Shao et al., 2016; Premoli et al., 2015; Saussine et al., 2015; Quinn et al., 2010).

2) Lowering the ballast profile

The vertical distance between the ballast bed surface and the top of the sleeper (aka. crosstie) is referred to as the "ballast profile". Given all other variables being equal, we compare flying ballast with two ballast profiles, 0 m from the top of the sleeper, and 0.04 m below the top of the sleeper. The point of interest is P1, which is the center track line. For the baseline scenario (profile = 0 m), the expected number of flying ballast particles is around 248 (Fig. 9). When the ballast profile is lowered by 0.04 m, the expected number of flying ballast particles would be reduced to 23. Reducing clearances between ballast and train will increase air speeds under trains and make ballast more vulnerable to aerodynamic effect. Railways thus tend to reduce the ballast shoulder and crib level with increased speed. A good ballast profile and avoiding ballast on the surface of the sleepers or bearers both help to reduce ballast flight. For example, the China HSR ballasted track standard reduces crib ballast level to 0.03–0.04 cm clearance with sleeper (250–300 km/h); however, this practice may reduce lateral track stability (Cléon, 2008).

3) Lowering the shoulder height

Only position P4 is discussed in this scenario. The simulated results are presented in Fig. 10. The result implies that ballast shoulder elevation influences the probability of ballast flight. More specifically, compared with the baseline scenario, when the ballast shoulder is lowered, the expectation of flying particles observed is sharply reduced (from 24 to 1).

When the shoulder height is set as level with other external ballasted areas or lowered, the phenomenon of ballast flight is effectively prevented. However, doing so results in lateral resistance insufficiency problems. Nowadays, operations on design ballasted tracks have increased speeds up to 320–360 km/h, and others even as high as 400 km/h. The above high-speed ballasted lines pose great challenges to ballast flight risk and track stability, whereas there are recent innovative ways available to increase sleeper lateral resistance, such as using dual-block or frictional sleepers, installing safety caps, or reconfiguring sleeper size and shape (Jing et al., 2012). Furthermore, the polyurethane system is one important optional method applied to ballasted HSR, especially for transition zones and bridges. For example, the ballast polyurethane used in China proves to be effective in engineering but lacks long-time maintenance data, such as tamping and maintenance interventions. It should be noted that ballast bagging is another risk mitigation strategy tested in Japan that needed to be removed and replaced for track maintenance (Jing et al., 2012).

In conclusion, the numerical simulation results are listed in Table 4.

6. Discussion

6.1. Effect of track position and speed on flying ballast risk

In general, the track centerline (P1) has a higher risk of ballast flight than other positions on the track (Fig. 11). Based on the previous discussion, this result is consistent with the distribution of aerodynamic load under the track section. In Fig. 11, the vertical

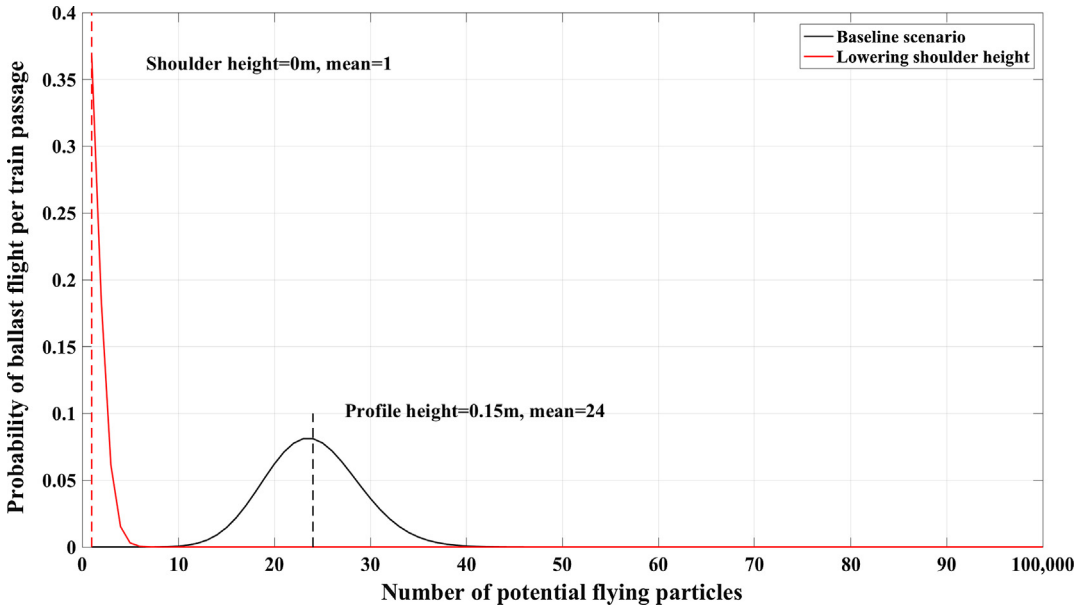

Fig. 10. Number of ballast flights per train passage at measured position P4.

Table 4
Averaged risk evaluation of ballast flight phenomenon.

Measured location velocity	P1 (profile height)		P2 (profile height)		P3 (profile height)		P4 (shoulder height)	
	0 m	−0.04 m	0 m	−0.04 m	0 m	−0.04 m	0.15 m	0 m
250 km/h	40	1	39	1	1	1	0	1
300 km/h	65	2	48	1	4	1	2	1
350 km/h	248	23	53	1	13	1	24	1
400 km/h	354	44	59	2	18	41	64	14

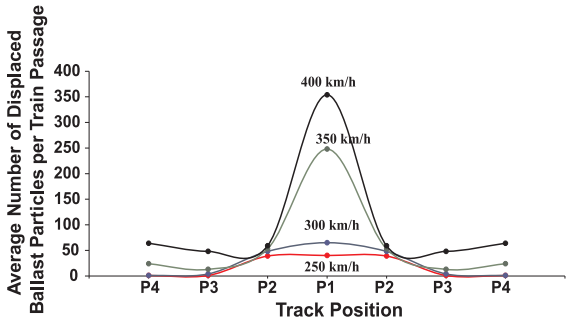

Fig. 11. Flying ballast risk (mean number of flying ballast particles) by track positions and speed on the studied HSR segment, with ballast profile at the top of sleeper and a ballast shoulder height of 0.15 m.

axis is represented by the average estimation of displaced particles per train passage.

From the result in Fig. 11, given track position, a higher train travel speed is associated with a higher risk. Also, given the speed, the track centerline has a higher flying ballast risk than other positions, probably due to aerodynamics caused by the train passages that significantly contribute to the release of particle movement (Saussine et al., 2015) and the fact that the peak value of aerodynamic force usually can be captured in the central area of the track bed (Quinn et al., 2010; Saat et al., 2015). For the position P1, Fig. 12 shows flying ballast risk given various speeds and ballast profile heights.

6.2. *Effect of ballast profile and speed*

Similar to Fig. 11, the vertical axis in Fig. 12 represents the average number of displaced particles per train passage. Based on the estimated results and the prior discussion, several risk mitigation strategies are identified as follows. For decision makers, the

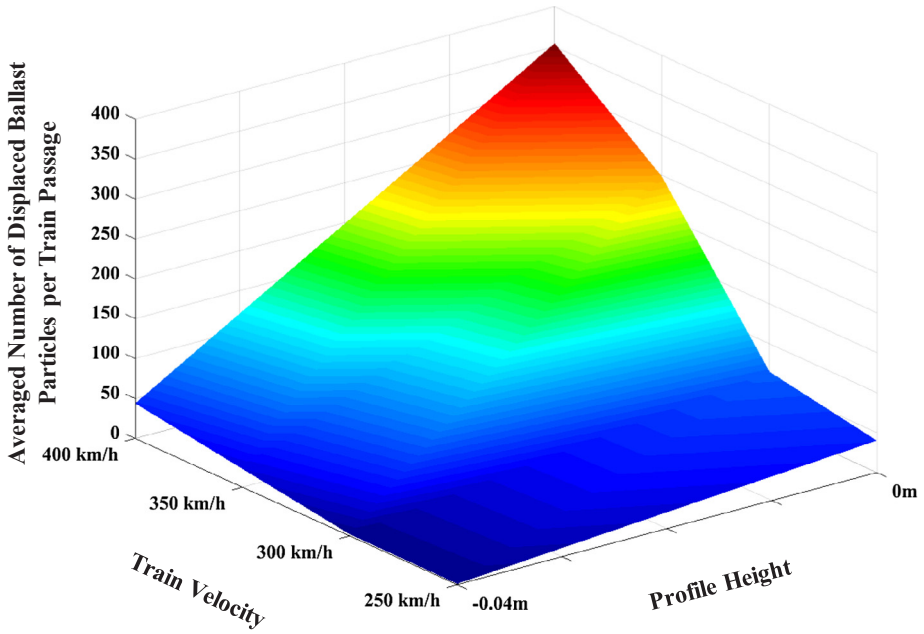

Fig. 12. Effect of ballast profile and speed on flying ballast risk (track centerline, P1).

management of flying ballast should be flexible, based on specific operating environment and conditions:

(a) When the traveling speed is around 400 km/h, the ballast flight probability reaches the highest level at all positions. Meanwhile, the phenomenon appears when the speed is over 300 km/h and becomes an important problem as the train velocity increases up to 350 km/h.
(b) Lowering the height of the ballasted area can greatly reduce the risk of particle flight. One possible explanation for this risk reduction is that lowering profile height contributes to a decrease in the aerodynamic loads on the ballasted bed surface, which plays a leading role in this phenomenon.
(c) While speed reduction and lowering ballast profile are expected to reduce flying ballast risk, they may affect train operational efficiency (speed reduction) and track lateral stability (lowered ballast profile). The scope of this paper focuses on evaluating the effectiveness of these risk reduction strategies on flying ballast risk. Separate future research should be conducted to understand the safety benefits, cost, and operational implications of risk reduction strategies.

7. Conclusions

This paper develops a Probabilistic Risk Analysis (PRA) model to understand flying ballast hazard on ballasted high-speed rail lines. The risk model accounts for track position, train speed, ballast degradation, ballast profile, and other factors. The analysis finds that flying ballast probability increases when train speed increases. Flying ballast probability would reduce when the ballast profile is lowered. In addition, flying ballast probability is expected to be higher in the centerline of the track than in other positions. Lowering ballast profile and shoulder height also leads to a reduction of flying ballast risk. However, both speed reduction and lowering ballast height have impacts on train operations or track stability. Ultimately, the model will be further developed into a multi-criteria decision analytic system that simultaneously considers the safety benefit and operational cost and impact of alternative risk mitigation strategies to optimize risk management decisions on high-speed rail systems.

8. Future work

(1) This paper focuses on the evaluation of a series of risk mitigation strategies with the application of a probabilistic risk assessment under specific scenarios. However, only the most common risk reduction methods are discussed in this paper due to data limitations.
(2) Also, this paper does not focus on evaluating the negative impact of each risk mitigation strategy on train operations and track stability. For example, speed reduction can reduce operational efficiency. Lowering ballast height can reduce track stability. The next step of this research will consider a variety of safety and economic impacts of these risk reduction strategies, individually or in combination, and account for both the investment in initial construction and the maintenance cost of long-term rehabilitation.
(3) Ultimately, a comprehensive risk management framework can be proposed to optimize the assignment of resources to minimize risk in the most cost-efficient manner and to generate better solutions for the management of safety concerns.

Acknowledgements

The first, second and fourth authors were partially funded by the USDOT Federal Railroad Administration when writing this paper. The third author was founded by the Natural Science Foundation of China (51578051). However, the authors are solely responsible for all the views and analyses herein.

References

American Society of Civil Engineers, 1994. Minimum design loads for buildings and other structures, Vol. 7. Amer Society of Civil Engineers.
Baker, C.J., 2010. The simulation of unsteady aerodynamic cross wind forces on trains. J. Wind Eng. Ind. Aerodyn. 98 (2), 88–99.
Baker, C.J., 2014. A review of train aerodynamics Part 2–applications. Aeronautical J. 118 (1202), 345–382.
Cali, P.M., Covert, E.E., 2000. Experimental measurements of the loads induced on an overhead highway sign structure by vehicle-induced gusts. J. Wind Eng. Ind. Aerodyn. 84 (1), 87–100.
Cléon, L.M., 2008. High-speed train. In: 8th World Congress on Railway Research, Seoul, Korea.
Cheli, F., Corradi, R., Diana, G., Ripamonti, F., Rocchi, D., Tomasini, G., 2007. Methodologies for assessing trains CWC through time-domain multibody simulations. In: Proceedings of the 12th International Conference on Wind Engineering, Cairns, Australia.
Esveld, C., Esveld, C., 2001. Modern Railway Track. MRT-Productions, Zaltbommel, The Netherlands.
Esveld, C., 2003. Recent developments in slab track. Eur. Railway Rev. 9 (2), 81–85.
Indraratna, B., Salim, W., Rujikiatkamjorn, C., 2011. Advanced Rail Geotechnology–Ballasted Track. CRC Press.
Ferreira, P.A., López-Pita, A., 2014. Improving ballasted high-speed railway track design for the reduction of vibration levels and maintenance needs (No. 14-4936).
Gao, Y., Qian, Y., Stoffels, S.M., Huang, H., Liu, S., 2017. Characterization of railroad crosstie movements by numerical modeling and field investigation. Constr. Build. Mater. 131, 542–551.
Garrick, B.J., Christie, R.F., 2002. Probabilistic risk assessment practices in the USA for nuclear power plants. Saf. Sci. 40 (1–4), 177–201.
Jacobini, F.B., Tutumluer, E., Saat, M.R., 2013. Identification of high-speed rail ballast flight risk factors and risk mitigation strategies. In: 10th World Congress on Railway Research, Sydney, Australia.
Jing, G.Q., Zhou, Y.D., Lin, J., Zhang, J., 2012. Ballast flying mechanism and sensitivity factors analysis. Int. J. Smart Sens. Intelligent Syst. 5 (4), 928–939.
Kaplan, S., Garrick, B.J., 1981. On the quantitative definition of risk. Risk Anal. 1 (1), 11–27.
Kwon, H.B., Park, C.S., 2006. An experimental study on the relationship between ballast-flying phenomenon and strong wind under high-speed-train. In: 7th World Congress on Railway Research. Montreal.
Kwon, S.D., 2010. Uncertainty of bridge flutter velocity measured at wind tunnel tests. In: The Fifth International Symposium on Computational Wind Engineering (CWE2010).
Lazaro, B., Gonzalez, E., Rodriguez, M., Osma, S., Iglesias, J., 2011. Characterization and modeling of flying ballast phenomena in high speed lines. In: 9th World Congress on Railway Research. Lille.
Luo, Y., Yin, H., Hua, C., 1996. The dynamic response of railway ballast to the action of trains moving at different speeds. Proc. Inst. Mech. Eng., Part F: J. Rail Rapid Transit 210 (2), 95–101.
Ministry of China Railway, 2008. Railway ballast.TB2140-2008 (In Chinese).
Mishra, D., Qian, Y., Huang, H., Tutumluer, E., 2014. An integrated approach to dynamic analysis of railroad track transitions behavior. Transportation Geotech. 1 (4), 188–200.
Mohaghegh, Z., Kazemi, R., Mosleh, A., 2009. Incorporating organizational factors into Probabilistic Risk Assessment (PRA) of complex socio-technical systems: A hybrid technique formalization. Reliab. Eng. Syst. Saf. 94 (5), 1000–1018.
Morgan, J.G.D., Markland, E., 1981. The effect of vibration on ballast beds. Geotechnique 31 (3), 367–386.
Paté-Cornell, E., 2002. Risk and uncertainty analysis in government safety decisions. Risk Anal. 22 (3), 633–646.
Paté-Cornell, E., Dillon, R., 2001. Probabilistic risk analysis for the NASA space shuttle: a brief history and current work. Reliab. Eng. Syst. Safety 74 (3), 345–352.
Pita, E.A.L., 2001. Ballast vibration makes new designs for high speed lines advisable. In: Proceedings of the 5th World Congress on Railways Research, Cologne, Germany.
Premoli, A., Rocchi, D., Schito, P., Somaschini, C., Tomasini, G., 2015. Ballast flight under high-speed trains: Wind tunnel full-scale experimental tests. J. Wind Eng. Ind. Aerodyn. 145, 351–361.
Prud'Home, A., 1970. La Voie Revue Generale des Chemins de Fer.
Quinn, A.D., Baker, C.J., Wright, N.G., 2001. Wind and vehicle induced forces on flat plates—Part 2: vehicle induced force. J. Wind Eng. Ind. Aerodyn. 89 (9), 831–847.
Quinn, A., Hayward, M., 2008. Full Scale Aerodynamic Measures Underneath A High Speed Train. BBAA VI International Colloquium, Milan.
Quinn, A., Hayward, M., Baker, C.J., Schmid, F., Priest, J.A., Powrie, W., 2010. A full-scale experimental and modelling study of ballast flight under high-speed trains. J. Rail Rapid Transit 61–74.
Saat, M.R., Bedini-Jacobini, F., Tutumluer, E., Barkan, C.P.L., 2015. Identification of high-speed rail ballast flight risk factors and risk mitigation strategies (No. DOT/FRA/ORD-15/03).
Saussine, G., Allain, E., Paradot, N., Gaillot, V., 2011. Ballast flying risk method for high speed line. In: 9th World Congress on Railway research. Lille.
Saussine, G., Allain, E., Vaillant, A., Ribourg, M., Neel, O., 2013. High Speed in Extreme Conditions: Ballast Projection Phenomenon. International Workshop on Train Aerodynamics, Birmingham.
Saussine, G., Voivret, C., Paradot, N., Allain, E., 2015. A risk assessment method for ballast flight; managing the rolling stock/infrastructure interaction. Proc. Inst. Mech. Eng., Part F: J. Rail Rapid Transit 229 (6), 581–593.
Shao, S., Jing, G., Yin, H., 2016. Ballast flight risk assessment based on reliability theory. Int. J. Simul.-Syst., Sci. Technol. 17 (36).
Steenbergen, M.J.M.M., Metrikine, A.V., Esveld, C., 2007. Assessment of design parameters of a slab track railway system from a dynamic viewpoint. J. Sound Vib. 306 (1), 361–371.
Soper, D., Baker, C., Jackson, A., Milne, D.R., Le Pen, L., Watson, G., Powrie, W., 2017. Full scale measurements of train underbody flows and track forces. J. Wind Eng. Ind. Aerodyn. 169, 251–264.
Vesely, W.E., Rasmuson, D.M., 1984. Uncertainties in nuclear probabilistic risk analyses. Risk Anal. 4 (4), 313–322.